



Iron Enhances Hepatic Fibrogenesis and Activates TGF- β Signaling in Murine Hepatic Stellate Cells

Q1 Kosha J. Mehta, PhD, Jason D. Coombes, PhD, Marco Briones-Orta, PhD,
 Q3 Q2 Paul P. Manka, MD, Roger Williams, MD, Vinood B. Patel, PhD and
 Q4 Wing-Kin Syn, MD



ABSTRACT

Introduction: Although excess iron induces oxidative stress in the liver, it is unclear whether it directly activates the hepatic stellate cells (HSC).

Materials and Methods: We evaluated the effects of excess iron on fibrogenesis and TGF- β signaling in murine HSC. Cells were treated with holotransferrin (0.005-5 g/L) for 24 hours, with or without the iron chelator deferoxamine (10 μ M). Gene expressions (α -SMA, *Col1- α 1*, *Serpine-1*, *TGF- β* , *Hif1- α* , *Tfrc* and *Slc40a1*) were analyzed by quantitative real time-polymerase chain reaction, whereas TfR1, ferroportin, ferritin, vimentin, collagen, TGF- β RII and phospho-Smad2 proteins were evaluated by immunofluorescence, Western blot and enzyme-linked immunosorbent assay.

Results: HSC express the iron-uptake protein TfR1 and the iron-export protein ferroportin. Holotransferrin upregulated TfR1 expression by 1.8-fold ($P < 0.03$) and ferritin accumulation (iron storage) by 2-fold ($P < 0.01$), and activated HSC with 2-fold elevations ($P < 0.03$) in α -SMA messenger RNA and collagen secretion, and a 1.6-fold increase ($P < 0.01$) in vimentin protein. Moreover, holotransferrin activated the TGF- β pathway with TGF- β messenger RNA elevated 1.6-fold ($P = 0.05$), and protein levels of TGF- β RII and phospho-Smad2 increased by 1.8-fold ($P < 0.01$) and 1.6-fold ($P < 0.01$), respectively. By contrast, iron chelation decreased ferritin levels by 30% ($P < 0.03$), inhibited collagen secretion by 60% ($P < 0.01$), repressed fibrogenic genes α -SMA (0.2-fold; $P < 0.05$) and TGF- β (0.4-fold; $P < 0.01$) and reduced levels of TGF- β RII and phospho-Smad2 proteins.

Conclusions: HSC express iron-transport proteins. Holotransferrin (iron) activates HSC fibrogenesis and the TGF- β pathway, whereas iron depletion by chelation reverses this, suggesting that this could be a useful adjunct therapy for patients with fibrosis. Further studies in primary human HSC and animal models are necessary to confirm this.

Key Indexing Terms: Fibrosis; Fibroblasts; Holotransferrin; Liver. [Am J Med Sci 2017;■(■):■■■-■■■.]

INTRODUCTION

Q8 During chronic liver injury, activation of hepatic stellate cells (HSC; the liver pericyte) occurs. This is characterized by upregulation of the HSC activation marker alpha smooth muscle actin (α -SMA) and increased expression of profibrogenic cytokines such as transforming growth factor- β (TGF- β). This invariably increases the expression of the mesenchymal marker vimentin and leads to the deposition of extracellular matrix components such as collagen to form a scar tissue, clinically referred to as fibrosis. Fibrosis reversibility may occur in early-stage disease, but it is less likely when scar tissues undergo cross-linking and become mature (i.e., advanced fibrosis).^{1,2} Therefore, targeting fibrosis during the early stages may prevent progression to cirrhosis (or advanced-stage chronic liver disease). However, despite the promising advances in the reversion of fibrosis and even cirrhosis to some extent in human³⁻⁵ and in animal models,^{6,7} mortality due to liver cirrhosis has doubled in the past 25 years. Liver transplantation remains the only curative option for end-stage cirrhosis, and approximately 60%

of liver transplantations are performed because of cirrhosis.⁸ Thus, further understanding of fibrogenic mechanisms is essential to help decelerate disease progression and increase the probability of regression.

"Fibrosis-promoting" chronic liver injury such as viral hepatitis, alcoholic liver disease and nonalcoholic fatty liver disease, often exhibit increased iron loading and deregulated iron metabolism.⁹⁻¹³ Unlike hereditary hemochromatosis, whereby specific mutations in iron-related genes lead to excessive systemic and cellular iron overload,¹⁴ it remains unclear whether excess iron is a mediator, or simply a marker of advanced liver fibrosis in the aforementioned etiologies. Under physiological conditions, iron is bound to its carrier protein transferrin, which delivers iron to cells by binding to the iron-uptake protein transferrin receptor (TfR)1 expressed on cell surfaces. Cellular iron-efflux, on the contrary, is mediated via the iron-exporter protein ferroportin, and excess iron is stored as ferritin. Under iron-excess conditions, when buffering capacities of the iron-binding proteins transferrin and ferritin are saturated, the excess "free," unbound iron accelerates the formation of reactive oxygen species in

the hepatocytes via the Fenton reaction, resulting in oxidative stress and hepatocyte injury.^{15,16} In turn, the damaged hepatocytes secrete cytokines and growth factors, which activate the HSC and promote fibrogenesis.^{17,18} However, apart from these indirect effects (i.e., iron induces hepatocyte oxidative stress), no study has yet reported whether iron can directly modulate the HSC phenotype in murine HSC.

Herein, we hypothesized that iron can directly regulate the HSC phenotype. Unlike previous studies that had used inorganic sources of iron such as ferric chloride or ferric chloride: citrate,^{19,20} we used holo-transferrin (holo-Tf) because it is the most physiological form of iron. Murine HSC were treated with a range of holo-Tf concentrations and core fibrogenic genes and proteins evaluated by quantitative real time-polymerase chain reaction (qRT-PCR), Western blot and the collagen-secretion assay. We assessed whether holo-Tf could regulate components of the TGF- β pathway and further examined if reduction of iron with the chelator deferoxamine (DFO) could inhibit iron-induced fibrogenic effects. Our studies show for the first time that the HSC express iron-transport proteins and that holo-Tf can directly activate HSC in part, via the TGF- β pathway. We further show that iron chelation reverses HSC fibrogenesis.

MATERIALS AND METHODS

Cell Culture and Treatments

The mouse HSC line (GRX) was maintained in Dulbecco's modified Eagle medium (Gibco, UK) with fetal calf serum, 1% penicillin-streptomycin (Gibco, UK) and 1% gentamycin (Gibco, UK). Trypsinization was performed with Tryple-E solution (Gibco, UK). Cells were treated with holo-Tf (Sigma Aldrich, UK) (0, 0.005, 0.05, 0.5, 2 and 5 g/L) for 24 hours and assessed for various parameters. In separate experiments, cells were treated with the iron chelator DFO (Sigma Aldrich, UK) (0, 0.1, 1, 10 and 100 μ M) for 24 hours and then harvested. In another set of experiments, referred to as the DFO double-dosage experiment, HSC were first treated with 0, 0.05, 0.5 and 2 g/L holo-Tf for 24 hours, and then supplemented with 10 μ M DFO for the next 24 hours. Following this period, HSC were further supplemented with 10 μ M DFO for an additional 24 hours. At the end of this 72-hour treatment period, cells were harvested and the parameters were assessed. Gene expressions (α -SMA, *Col1- α 1*, *Serpine-1*, *TGF- β* , *Hif1- α* , *Tfrc* and *Slc40a1*) were analyzed by qRT-PCR, whereas TfR1, ferroportin, ferritin, vimentin, collagen, TGF- β RII and phospho-Smad2 proteins were examined by immunofluorescence, Western blot and enzyme-linked immunosorbent assay.

Immunofluorescence for Iron-Transport Proteins

The cellular iron-uptake protein TfR1 and the iron-export protein ferroportin were detected by

immunofluorescence. Briefly, cells were fixed in 4% formaldehyde for 10 minutes at room temperature, blocked with 1% bovine serum albumin in 0.1% phosphate-buffered saline (PBS)-tween and then probed with rabbit anti-TfR1 antibody (5 μ g/mL, Abcam AB84036) or rabbit anti-ferroportin antibody (10 μ g/mL, Abcam, AB85370), as per manufacturer's instructions. Fluorescence detection was achieved by using a secondary goat anti-Rabbit Alexa Fluor 488 antibody (2 μ g/mL, Abcam).

Gene Expression Analysis

Cells were washed with PBS and treated with Trizol reagent (Sigma Aldrich, UK) (500 μ L per well), and RNA was extracted as per manufacturer's instructions. Complementary DNA (cDNA) synthesis of 1,000 ng RNA was conducted using iScript cDNA Synthesis Kit (Biorad, UK), as recommended by the manufacturer. The messenger RNA (mRNA) expressions of the genes *Serpine-1*, *Col1- α 1*, α -SMA, *TGF- β* and *Hif1- α* were normalized to *s9* expression (Supplementary Table S1 online).^{21,22} Gene expression was measured using Applied Biosystems 7500, and the data were analyzed by the relative quantification method, Delta-Delta Ct ($\Delta\Delta$ Ct), and expressed as $2^{-\Delta\Delta$ Ct}.²³

Ferritin Level Measurements

Cells were washed with PBS and lysed with lysis buffer (radioimmunoprecipitation assay buffer [Sigma Aldrich, UK] and Complete-Mini-protease inhibitor cocktail tablet [Roche, UK]), as per manufacturer's instructions. Samples were collected on ice, vortexed for 3 seconds and ferritin levels measured using a mouse ferritin enzyme-linked immunosorbent assay kit (Abcam, UK). Levels were normalized to protein concentration measured by Precision Red (CycloSystem, USA).

Western Blot

Cells were washed with PBS and lysed with radioimmunoprecipitation assay buffer (Sigma Aldrich, UK) containing Complete-Mini Protease inhibitor cocktail (Roche, UK) and Phospho-stop (Roche, UK), as per manufacturer's instructions. Cell extracts were centrifuged for 5 minutes at 14,000 rotations/minute, and the supernatant was electrophoresed on Novex Blot 4-12% Bis-Tris gels as per the Novex Bolt system (Thermo-Fisher Scientific, UK). Following protein transfer to polyvinylidene difluoride or nitrocellulose membrane via the iBlot system (Invitrogen, UK), membranes were probed with primary antibodies (1:1,000) overnight in a cold room, followed by treatment with appropriate horseradish peroxidase-conjugated detection antibodies (1:10,000) for 1 hour, at room temperature on shaker (Supplementary Table 2 online). Protein bands were observed on the ChemiDoc imager (Biorad, UK) and analyzed using the Image lab software (Biorad, UK).

Protein density was analyzed by the Image-J software available at the National Institutes of Health.

Viability Assay and Collagen Secretion

For viability studies, cells were first seeded at a density of 5×10^3 cells/well in 96-well plates. After 24 hours of treatment with holo-Tf, viability was measured by using the CCK-8 kit (Dojindo Laboratories, Japan), as per the manufacturer's instructions. Secreted collagen was measured in cell-conditioned media. Cells were first seeded in a 6-well plate. Following holo-Tf treatments, conditioned media were collected and collagen measured using the Sircol assay (Bicolor, UK). Levels were normalized to protein concentration measured by Precision Red (CycloSystem, USA).

Statistical Analysis

Data were analyzed using student's *t*-test (two-tailed distribution, 2 sample and unequal variance). The level of significance was set at $P < 0.05$. Data were presented as mean \pm standard deviation (n : 3-9), and statistical analyses are based on n values.

RESULTS

HSC Expressed Iron-Transport Proteins and Responded to Exogenous Iron

Mouse HSC expressed the cellular iron-uptake protein TfR1 (Figure 1A) and the iron-export protein ferroportin (Figure 1B). Basal mRNA expression of the core fibrogenic genes *Serpine-1*, *Col1- α 1* and α -SMA, and the key iron-transport genes *Tfrc* and *Slc40a1* in the HSC are shown in Figure 1C. To assess whether HSC would respond to exogenous iron, cells were treated with holo-Tf, the physiological relevant form of iron. Holo-Tf significantly upregulated the expression of the iron-uptake protein TfR1 (holo-Tf 0.05 g/L: 1.7-fold, $P < 0.03$; holo-Tf 0.5 g/L: 1.8-fold, $P < 0.03$; holo-Tf 2 g/L: 1.7-fold, $P < 0.05$) (Figure 1D). As the greatest induction of fibrogenic genes *Serpine-1* and α -SMA occurred 24 hours posttreatment (Supplementary Figure 1 online), HSC were treated with holo-Tf for 24 hours in all subsequent experiments. To determine whether holo-Tf treatment led to accumulation of cellular iron, we measured levels of the iron-storage protein ferritin. Results demonstrate that treatment with holo-Tf resulted in a dose-dependent accumulation of cellular iron: treatment with 0.005 g/L of holo-Tf increased ferritin by 1.6-fold ($P < 0.01$), and treatment with 5 g/L of holo-Tf increased ferritin by 2-fold ($P < 0.01$) (Figure 1E).

Holo-Tf Activated HSC and Induced Deposition of the Extracellular Matrix Collagen

As HSC expressed iron-transport proteins and responded to exogenous iron by increasing cellular iron (Figures 1A and 1E), we next examined whether iron accumulation was associated with HSC activation.

Accordingly, HSC were treated with holo-Tf for 24 hours and then harvested for mRNA and protein analysis. We found that holo-Tf upregulated the HSC activation marker, α -SMA, by up to 2-fold ($P < 0.03$) (Figure 2A), and the profibrogenic marker and TGF- β target gene, *serpine-1*, by up to 2.5-fold ($P < 0.05$) (Figure 2B).

Furthermore, holo-Tf treatment induced collagen secretion into the conditioned media by up to 1.9-fold ($P < 0.03$) (Figure 2C) and increased vimentin protein levels by up to 1.6-fold ($P < 0.01$) upon 0.5 g/L holo-Tf treatment (Figure 2D and Supplementary Figure 2 online). Previous studies had reported that iron could mediate its effects via the hypoxia-inducible factor 1, alpha subunit (HIF1 α).²⁴ Herein, we observed that holo-Tf induced Hif1 α expression by up to 1.9-fold ($P < 0.05$) after 24 hours (Supplementary Figure 2 online). The addition of holo-Tf however, had no effect on HSC viability (Supplementary Figure 2 online).

Holo-Tf Upregulated TGF- β mRNA and Promoted TGF- β Signaling

The fibrotic liver microenvironment is enriched with profibrogenic factors.²⁵ As TGF- β is the prototypical profibrogenic cytokine and is overexpressed in the fibrotic liver tissue,²⁶ we examined whether holo-Tf enhanced TGF- β signaling. Data showed that holo-Tf upregulated TGF- β mRNA expression (holo-Tf 0.005 g/L: 1.2-fold, $P = 0.05$; holo-Tf 0.05 g/L: 1.7-fold, $P = 0.07$; holo-Tf 0.5 g/L: 1.6-fold, $P = 0.05$) (Figure 3A), and it also increased protein levels of the TGF- β receptor TGF- β RII by up to 1.8-fold ($P < 0.01$) (Figure 3B) and phospho-Smad 2 by up to 1.6-fold ($P < 0.01$) (Figure 3C). Collectively, the data suggest that holo-Tf directly activated the HSC via the canonical TGF- β signaling.

Iron Chelation Abrogated Iron-Induced Fibrogenesis and Inhibited TGF- β Signaling

DFO treatment has been successfully used in patients with hemochromatosis (iron overload).²⁷ Having shown that exogenous iron could promote TGF- β signaling and activate HSC (Figures 2 and 3), we next tested whether iron depletion with DFO inhibits HSC activation. To determine the most appropriate concentration of DFO for iron depletion experiments, HSC were treated with a range of DFO concentrations for 24 hours. Results showed significantly reduced ferritin levels ($P < 0.03$) when HSC were treated with the lowest DFO concentration (0.1 μ M), and this level of reduction was maintained across all other DFO concentrations (Figure 4A). In addition, iron chelation was associated with >50% reductions ($P < 0.05$) in α -SMA mRNA (Figure 4B), TGF- β mRNA (Supplementary Figure 3 online), *Col1- α 1* mRNA (Figure 4C), and in the levels of secreted collagen (Figure 4C).

Next, we determined whether DFO could inhibit holo-Tf-induced HSC fibrogenesis. Based on earlier

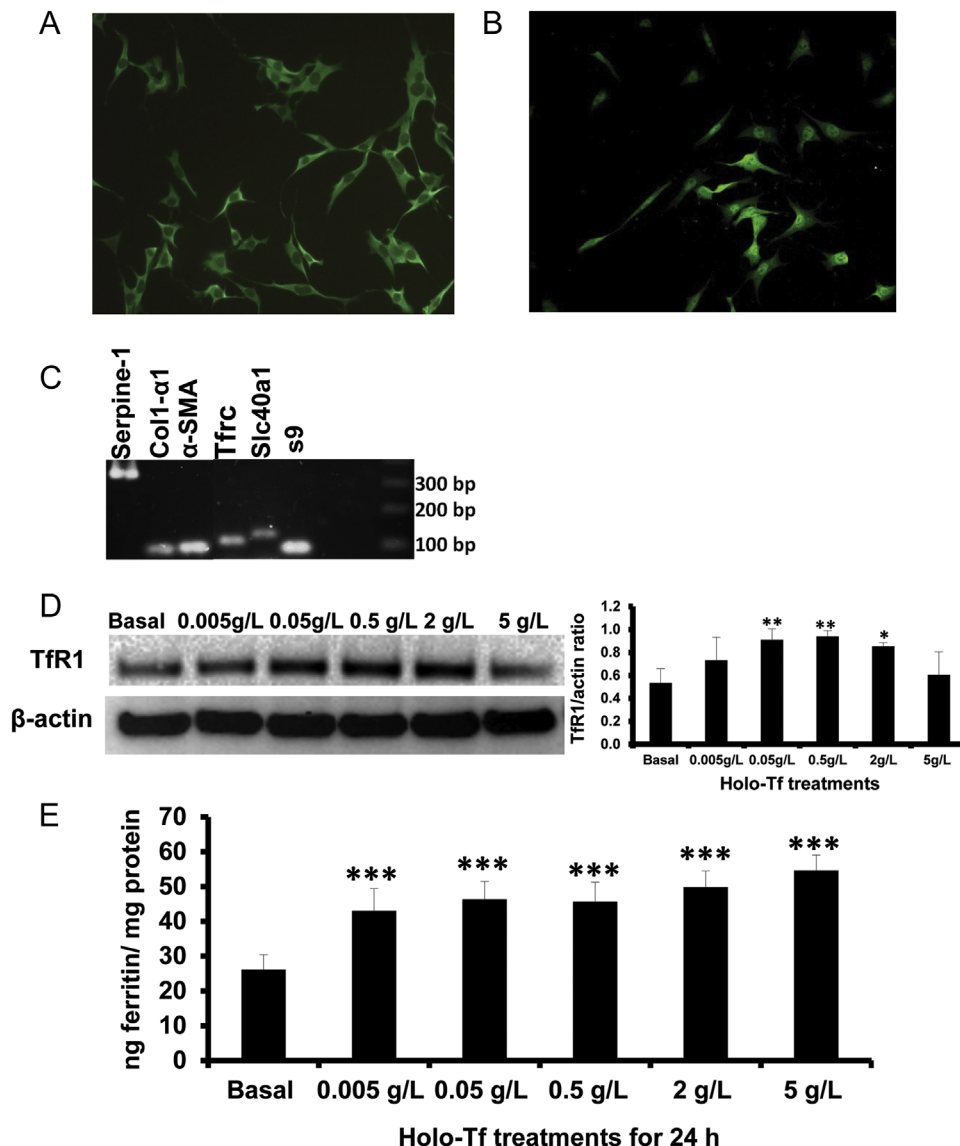


FIGURE 1. Expression of iron transport and storage proteins in murine HSC. Murine HSC were used, and expression of iron transport or storage proteins was evaluated by immunofluorescence (IF), qRT-PCR and Western blot. (A) Iron import protein Tfr1 by IF; (B) the iron-export protein ferroportin by IF; (C) 1% agarose gel image of cDNA amplicons obtained during qRT-PCR: *Serpine-1*, *Col1-α1*, *α-SMA*, *Tfr1*, *Slc40a1* and the housekeeping gene *s9*, respectively; (D) Western blot of Tfr1 and corresponding densitometry following holo-Tf treatment for 24 hours; (E) levels of ferritin (the iron storage protein) by ELISA following holo-Tf treatment for 24 hours. Data are presented as mean \pm SD. * $P < 0.05$, ** $P < 0.03$ and *** $P < 0.01$ compared to basal conditions. ELISA, enzyme-linked immunosorbent assay; SD, standard deviation.

findings (Figure 4 and Supplementary Figure 3 online), HSC were treated with a combination of 10 μ M DFO and holo-Tf (0.05, 0.5 and 2 g/L) for 24 hours. Furthermore, 10 μ M DFO was used because this was the lowest concentration that significantly repressed collagen mRNA and protein secretion (Figures 4C and 4D). As we did not observe any significant response with this (Supplementary Figure 4 online), we proceeded with the DFO double-dosage experiment, as explained in Methods. Briefly, HSC were first treated with holo-Tf for 24 hours, then supplemented with 10 μ M DFO twice, for 24 hours each time, and then harvested after the 72-hour

treatment period. For DFO double-dosage experiments, we excluded the lowest and the highest dosages of 0.005 and 5 g/L holo-Tf, respectively, because these are physiologically less relevant, and holo-Tf concentration ranges from 0.05-2 g/L and more closely represents the low-to-moderate iron-excess conditions seen in non-hereditary iron-loaded conditions.

Results showed that DFO double-dosage treatment significantly reduced iron-induced ferritin levels by 30% ($P < 0.03$) (Figure 5A). Holo-Tf-induced collagen secretion was also reduced by up to 60% ($P < 0.01$) (Figure 5B). Moreover, *α-SMA* and *Col1-α1* mRNA were

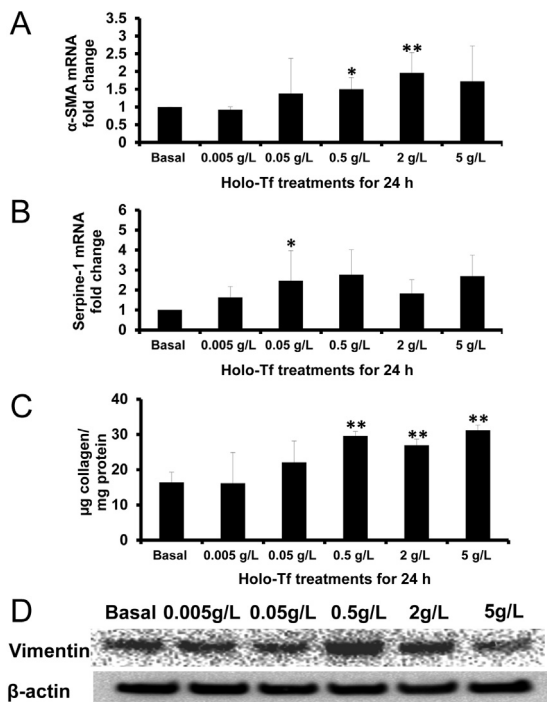


FIGURE 2. Exogenous iron activated murine HSC. Mouse HSC were treated with holo-Tf for 24 hours. HSC were then harvested for RNA and protein analysis by qRT-PCR and Western blot, respectively; conditioned media was collected for collagen secretion assay. (A) α -SMA mRNA. (B) *Serpine-1* mRNA. (C) Collagen secretion into conditioned media as measured by the Sircol assay. (D) Vimentin by Western blot. Data are presented as mean \pm SD. * $P < 0.05$ and ** $P < 0.03$ compared to basal conditions. SD, standard deviation.

significantly repressed by up to 80% ($P < 0.05$) and 30% ($P < 0.03$), respectively (Figures 5C and 5D). Similarly, *TGF- β* and *Hif1- α* mRNA were also significantly downregulated by up to 60% ($P < 0.01$) and 50% ($P < 0.03$), respectively (Supplementary Figure 5 online). The DFO double-dosage treatment also decreased the iron-induced levels of TGF- β RII (Figure 6A) and phospho-Smad2 (Figure 6B), components of the TGF- β pathway.

DISCUSSION

Although the role of excess iron in mediating hepatocyte damage is well established,¹⁸ its effect on HSC phenotype and function remains poorly understood. Herein, we provide compelling evidence to confirm that excess iron directly enhances HSC fibrogenesis in part, through TGF- β activation, and that iron chelation reverses this.

In this study, we have comprehensively evaluated the fibrogenic response in a mouse HSC line.^{19,20,28} HSC were treated with a range of holo-Tf and DFO concentrations, and multiple fibrosis-associated genes and proteins evaluated by qRT-PCR, Western blot and collagen secretion assays. We found that iron loading

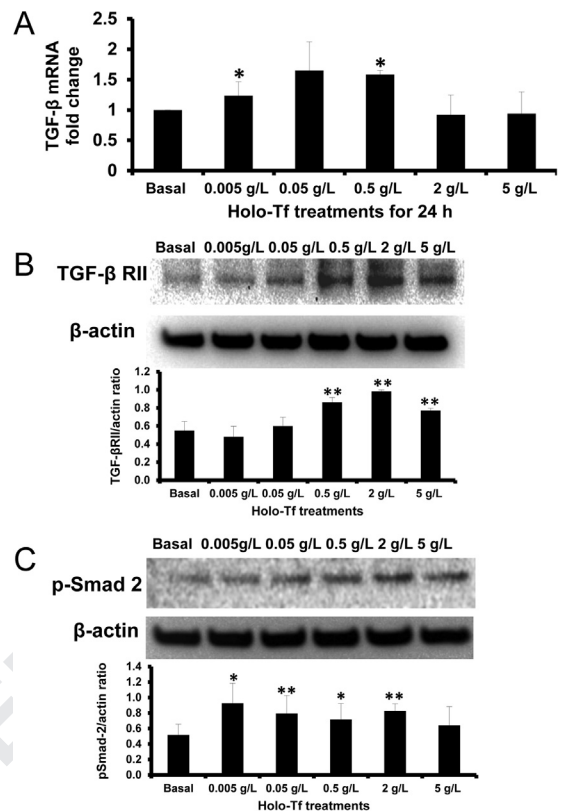


FIGURE 3. Iron loading activated the TGF- β pathway in murine HSC. HSC were treated with holo-Tf for 24 hours and then harvested for RNA and protein analysis by qRT-PCR and Western blot. (A) TGF- β mRNA; (B) TGF- β RII Western blot and densitometry; and (C) phospho-Smad 2 Western blot and densitometry. Data are presented as mean \pm SD. * $P \leq 0.05$ and ** $P < 0.03$ compared to basal conditions. SD, standard deviation.

directly activated HSC significantly; holo-Tf treatment upregulated α -SMA, increased vimentin levels and induced collagen secretion. Conversely, treatment with the iron chelator inhibited or reversed the fibrogenic phenotype. We also demonstrated for the first time that the HSC express key iron transporters; the iron-uptake protein TfR1 and the iron-storage protein ferritin. In contrast to previous reports,^{19,20,28} we further confirmed that holo-Tf induced intracellular iron accumulation (ferritin levels), and that iron chelation reduced HSC (i.e., cellular) iron under both basal and holo-Tf supplemented conditions. These results imply that the changes in fibrogenesis observed with holo-Tf treatment and iron chelation could be attributed to differences in cellular iron levels. The cause(s) for the apparent "saturation" of ferritin levels (iron accumulation) upon holo-Tf treatment (Figure 1E) is not known, but may be related to the saturation of transferrin receptors on cell surfaces (which prevented further iron uptake), or the cellular iron regulatory mechanisms exhibited by the iron response elements on *Tfrc* transcripts that prevent its translation to TfR1 protein under intracellular iron-replete state, thereby limiting further iron acquisition.²⁹ In addition,

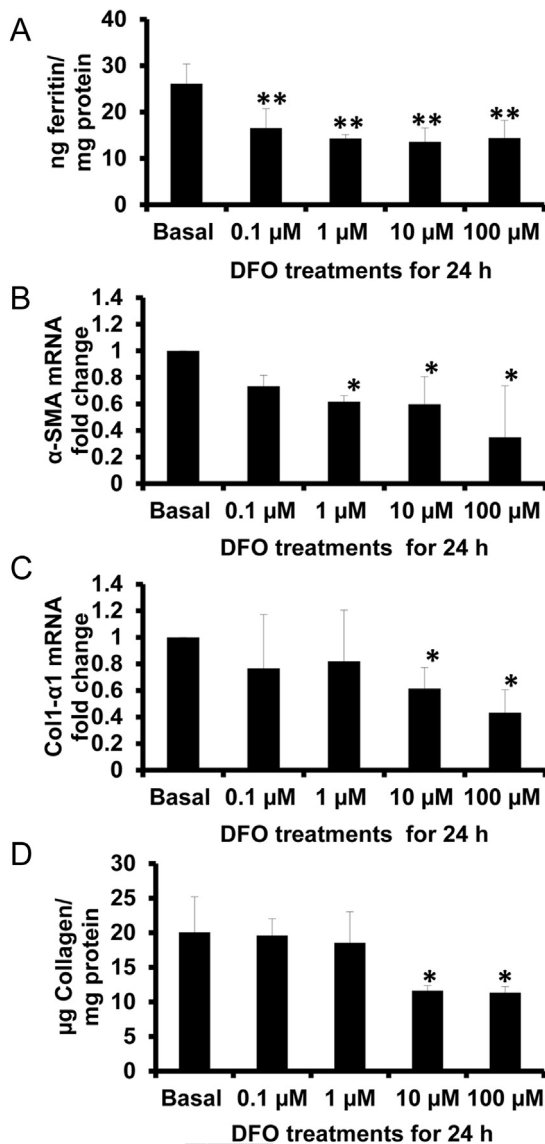


FIGURE 4. Iron chelation repressed fibrotic responses in murine HSC. Mouse HSC cultures were treated with a range of DFO concentrations for 24 hours. At the end of treatment, HSC were harvested and cellular iron levels (ferritin) measured by ELISA, RNA analyzed by qRT-PCR and collagen secretion into conditioned media assessed by the Sircoll assay. (A) Ferritin levels by ELISA; (B) α -SMA mRNA; (C) *Col1- α 1* mRNA; and (D) collagen secretion into conditioned media. Data are presented as mean \pm SD. * P < 0.05 and ** P \leq 0.03 compared to basal conditions. ELISA, enzyme-linked immunosorbent assay; SD, standard deviation.

we noted that the holo-Tf upregulated *TGF- β* mRNA, and increased expression *TGF- β* RII and phospho-Smad2, thereby demonstrating that holo-Tf activates *TGF- β* signaling, a key profibrogenic cytokine that is highly expressed in chronic liver disease.³⁰ Conversely, iron depletion by the chelator attenuated *TGF- β* signaling. Collectively, these novel data suggest that iron-induced fibrogenesis could be mediated at least in part, by

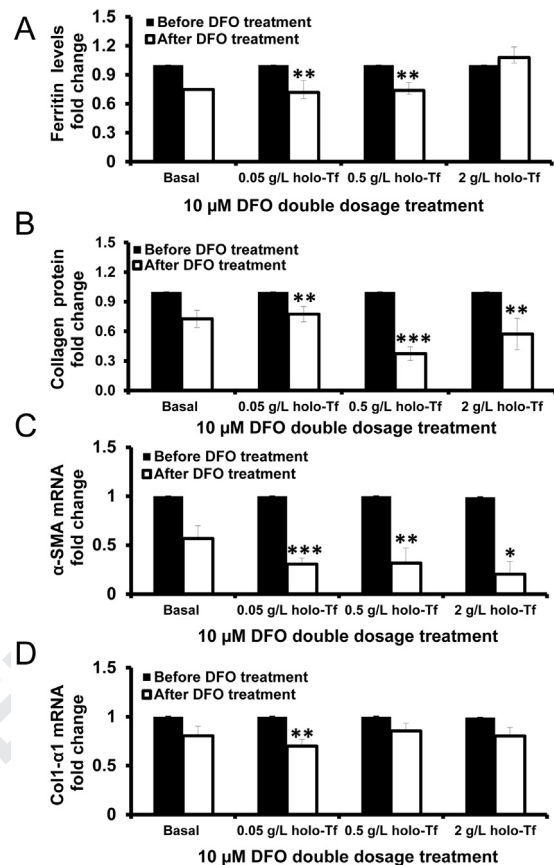


FIGURE 5. Iron chelation reduced iron-induced ferritin levels and attenuated fibrotic responses in murine HSC. Mouse HSC were first treated with 0, 0.05, 0.5 and 2 g/L holo-Tf for 24 hours and then supplemented with 10 μM DFO for the next 24 hours. Following this period, HSC were further supplemented with 10 μM DFO for an additional 24 hours. At the end of this 72-hour treatment period, cells were harvested and cellular iron levels measured by ELISA, RNA analyzed by qRT-PCR and collagen secretion into conditioned media assessed by the Sircoll assay. (A) Ferritin levels by ELISA; (B) collagen secretion by the Sircoll assay; (C) α -SMA mRNA; and (D) *Col1- α 1* mRNA. Data are presented as mean \pm SD. * P < 0.05, ** P < 0.03 and *** P < 0.01 compared to basal conditions. ELISA, enzyme-linked immunosorbent assay; SD, standard deviation.

activation of canonical *TGF- β* signaling. Thus, excess iron-induced HSC activation can potentially amplify free-iron-mediated hepatocyte oxidative stress that lead to progressive liver fibrosis.³¹

In this study, cells were treated with a wide range of holo-Tf concentration (from 0.005-5 g/L) that represents normal physiological range (2-3 g/L) as well as the ranges of transferrin observed during pathological conditions such as iron deficiency and iron overload. If we assume the mean iron saturation of 30% and amount of transferrin as 2 g/L, then the amount of iron-loaded transferrin equates to 0.6 g/L. In the setting of hemochromatosis, between 45% and 50% of transferrin is iron-saturated, which then accounts for 1.4-1.5 g/L of iron-loaded transferrin. Therefore, the concentrations of

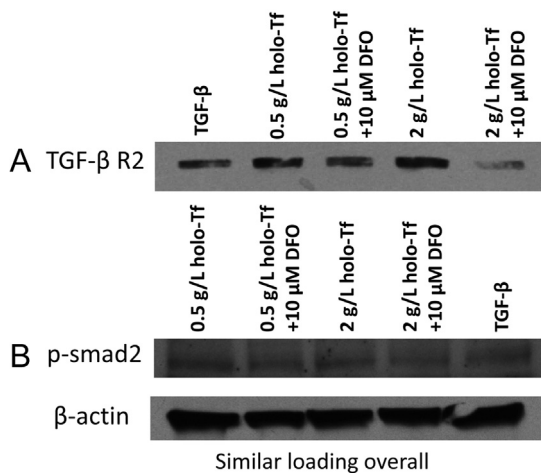


FIGURE 6. Iron chelation inhibited TGF- β signaling in murine HSC. Mouse HSCs were treated as described in Fig 5. Cells were then harvested and protein expression evaluated by Western blot. (A) TGF- β RII and (B) phospho-Smad 2. Beta actin was used as loading control.

holo-Tf used in this study (i.e., 0.5–5 g/L) represent both normal to pathological states. We anticipated that the highest level of holo-Tf (i.e., 5 g/L) concentration could lead to outlier and unexpected responses, but felt that this had to be studied to test this hypothesis. For example, holo-Tf-induced upregulations in TfR1 (Figure 1D), vimentin (Figure 2D), TGF- β RII (Figure 3B) and psmad-2 (Figure 3C) occurred only at concentrations at, or below 2 g/L holo-Tf; treatment with 5 g/L holo-Tf, by contrast, led to repression of these responses. We also studied cell responses to significantly lower concentrations of holo-Tf (0.005 and 0.05 g/L) to determine whether there was a dose-dependent response.

Unlike previous studies that had only evaluated the effects of DFO under basal conditions (i.e., without holo-Tf treatment),¹⁹ this study also evaluated the effects of DFO on HSC under conditions of “iron-overload” (i.e., holo-Tf treated HSC). The observation that DFO could inhibit HSC fibrogenesis under conditions of “iron-overload” is clinically significant because this suggests that iron chelation could potentially be used to treat individuals with alcoholic liver disease or nonalcoholic fatty liver disease/nonalcoholic steatohepatitis fibrosis and concomitant low-moderate iron overload^{14,32} (i.e., a useful adjunct therapy to reduce liver fibrosis in those with chronic liver diseases). DFO is currently being used to treat individuals with iron overload from genetic hemochromatosis and is effective in reducing inflammation and atherosclerosis in murine models.³³ The combination of DFO and deferriprone (another iron chelator) has also been shown to be effective in reducing intracellular iron pool and transferrin saturation.^{34,35} Thus, iron chelation therapy could potentially be translated to the bedside to treat liver fibrosis.

Interestingly, following the DFO double-dosage treatment, secreted collagen (protein) was significantly

reduced when treated with DFO (all concentrations) (Figure 5B), but gene expression changes were only statistically significant under low holo-Tf concentrations (i.e., 0.05 g/L; Figure 5D). This could be explained, in part, by the relatively reduced effects of DFO under “high iron” conditions or a lag between transcription and translation/secretion responses at various iron concentrations (i.e., mRNA changes occurred quickly and then returned to basal levels while protein changes are yet to occur). The latter could also be explained by variations in mRNA or protein stability or rate of mRNA degradation. More likely, however, this is because we are measuring protein *already secreted* out of cells into the conditioned media (and stable), while gene expression is dynamic.

Hypoxia has been implicated in the development of several liver diseases because the gradient of oxygen through the hepatic lobule greatly affects the functions of the hepatic cells.²⁴ Although hypoxia modulates iron homeostasis through hypoxia-inducible factors (HIFs),^{24,29,36} several fibrosis-associated HIF-target genes have been identified, such as *serpine-1* and *prolyl-4 hydroxylase α 2*,³⁷ thus suggesting a link between iron homeostasis and fibrosis via HIFs. Unsurprisingly, HIF-1 α has been shown to enhance the fibrogenic responses.^{37–39} This study demonstrated an upregulation of *Hif-1 α* mRNA upon holo-Tf treatments, followed by its repression upon DFO treatment, which suggests that the antifibrotic effects of DFO may be through the modulation of HIF-1 α levels. Further studies will be needed to identify additional HIF-regulated fibrogenic and iron-related genes that could be developed as targets for antifibrotic therapies. Additional experiments using primary human HSC and animal models of liver fibrosis are also needed to confirm these DFO-mediated antifibrotic effects.

CONCLUSIONS

We confirm a direct connection between iron and fibrosis. Our data show that iron can directly activate the TGF- β pathway and directly promote liver fibrosis, whereas iron depletion with DFO can reverse this by reducing intracellular iron, thereby inhibiting TGF- β signaling, and repressing fibrogenesis. Therefore, iron chelation may be a useful adjunctive therapy to inhibit liver fibrosis progression.

ACKNOWLEDGMENTS

GRX was kindly provided by Professor J Oliveira (Brazil).

Appendix A. Supporting information

Supplementary data associated with this article can be found in the online version at <http://dx.doi.org/10.1016/j.amjms.2017.08.012>.

REFERENCES

1. **Moreira RK.** Hepatic stellate cells and liver fibrosis. *Arch Pathol Lab Med* 2007;131(11):1728–34.
2. **Li D, Friedman SL.** Liver fibrogenesis and the role of hepatic stellate cells: new insights and prospects for therapy. *J Gastroenterol Hepatol* 1999;14(7):618–33.
3. **D'Ambrosio R, Aghemo A, Rumi MG, et al.** A morphometric and immunohistochemical study to assess the benefit of a sustained virological response in hepatitis C virus patients with cirrhosis. *Hepatology* 2012;56(2):532–43.
4. **McPherson S, Hardy T, Henderson E, et al.** Evidence of NAFLD progression from steatosis to fibrosing-steatohepatitis using paired biopsies: implications for prognosis and clinical management. *J Hepatol* 2015;62(5):1148–55.
5. **Marcellin P, Gané E, Buti M, et al.** Regression of cirrhosis during treatment with tenofovir disoproxil fumarate for chronic hepatitis B: a 5-year open-label follow-up study. *Lancet* 2013;381(9865):468–75.
6. **Sobrevals L, Rodríguez C, Romero-Trejejo JL, et al.** Insulin-like growth factor I gene transfer to cirrhotic liver induces fibrolysis and reduces fibrogenesis leading to cirrhosis reversion in rats. *Hepatology* 2010;51(3):912–21.
7. **Kisseleva T, Cong M, Paik Y, et al.** Myofibroblasts revert to an inactive phenotype during regression of liver fibrosis. *Proc Natl Acad Sci U S A* 2012;109(24):9448–53.
8. **Manns MP.** Liver cirrhosis, transplantation and organ shortage. *Dtsch Arztebl Int* 2013;110(6):83–4.
9. **Milic S, Mikolasevic I, Orlic L, et al.** The role of iron and iron overload in chronic liver disease. *Med Sci Monit* 2016;22:2144–51.
10. **Fujita N, Takei Y.** Iron overload in nonalcoholic steatohepatitis. *Adv Clin Chem* 2011;55:105–32.
11. **Nelson JE, Klintworth H, Kowdley KV.** Iron metabolism in nonalcoholic fatty liver disease. *Curr Gastroenterol Rep* 2012;14(1):8–16.
12. **Sebastiani G, Tempesta D, Alberti A.** Hepatic iron overload is common in chronic hepatitis B and is more severe in patients coinfecting with hepatitis D virus. *J Viral Hepat* 2012;19(2):e170–6.
13. **Rouault TA.** Hepatic iron overload in alcoholic liver disease: why does it occur and what is its role in pathogenesis? *Alcohol* 2003;30(2):103–6.
14. **Pietrangolo A.** Hereditary hemochromatosis: pathogenesis, diagnosis, and treatment. *Gastroenterology* 2010;139(2):393–408, 408.e1–2.
15. **Pietrangolo A.** Metals, oxidative stress, and hepatic fibrogenesis. *Semin Liver Dis* 1996;16(1):13–30.
16. **Lemire JA, Harrison JJ, Turner RJ.** Antimicrobial activity of metals: mechanisms, molecular targets and applications. *Nat Rev Microbiol* 2013;11(6):371–84.
17. **Fauzi S, Lepreux S, Bedin C, et al.** Activation of cultured rat hepatic stellate cells by tumoral hepatocytes. *Lab Invest* 1999;79(4):485–93.
18. **Philippe M-A, Ruddell R-G, Ramm G-A.** Role of iron in hepatic fibrosis: one piece in the puzzle. *World J Gastroenterol* 2007;13(35):4746–54.
19. **Jin H, Terai S, Sakaida I.** The iron chelator deferoxamine causes activated hepatic stellate cells to become quiescent and to undergo apoptosis. *J Gastroenterol* 2007;42(6):475–84.
20. **Gardi C, Arezzini B, Fortino V, et al.** Effect of free iron on collagen synthesis, cell proliferation and MMP-2 expression in rat hepatic stellate cells. *Biochem Pharmacol* 2002;64(7):1139–45.
21. **Coombes JD, Swiderska-Syn M, Dollé L, et al.** Osteopontin neutralisation abrogates the liver progenitor cell response and fibrogenesis in mice. *Gut* 2015;64(7):1120–31.
22. **Scotland PB, Heath JL, Conway AE, et al.** The PICALM protein plays a key role in iron homeostasis and cell proliferation. *PLoS One* 2012;7(8): e34133. [cited June 30, 2016]. <http://www.ncbi.nlm.nih.gov/pmc/articles/PMC3431333/>.
23. **Livak KJ, Schmittgen TD.** Analysis of relative gene expression data using real-time quantitative PCR and the 2(-Delta Delta C(T)) method. *Bioinformatics* 2001;25(4):402–8.
24. **Peyssonaux C, Nizet V, Johnson RS.** Role of the hypoxia inducible factors HIF in iron metabolism. *Cell Cycle* 2008;7(1):28–32.
25. **Lee UE, Friedman SL.** Mechanisms of hepatic fibrogenesis. *Best Pract Res Clin Gastroenterol* 2011;25(2):195–206.
26. **Dooley S, ten Dijke P.** TGF- β in progression of liver disease. *Cell Tissue Res* 2012;347(1):245–56.
27. **Nielsen P, Fischer R, Buggisch P, et al.** Effective treatment of hereditary haemochromatosis with desferrioxamine in selected cases. *Br J Haematol* 2003;123(5):952–3.
28. **Bridle KR, Crawford DHG, Ramm GA.** Identification and characterization of the hepatic stellate cell transferrin receptor. *Am J Pathol* 2003;162(5):1661–7.
29. **Muckenthaler MU, Galy B, Hentze MW.** Systemic iron homeostasis and the iron-responsive element/iron-regulatory protein (IRE/IRP) regulatory network. *Annu Rev Nutr* 2008;28:197–213.
30. **Ranganathan P, Agrawal A, Bhushan R, et al.** Expression profiling of genes regulated by TGF-beta: differential regulation in normal and tumour cells. *BMC Genomics* 2007;8:98.
31. **Jomova K, Valko M.** Importance of iron chelation in free radical-induced oxidative stress and human disease. *Curr Pharm Des* 2011;17(31):3460–73.
32. **Bacon BR, Adams PC, Kowdley KV, et al. American Association for the Study of Liver Diseases.** Diagnosis and management of hemochromatosis: 2011 practice guideline by the American Association for the Study of Liver Diseases. *Hepatology* 2011;54(1):328–43.
33. **Zhang W-J, Wei H, Frei B.** The iron chelator, desferrioxamine, reduces inflammation and atherosclerotic lesion development in experimental mice. *Exp Biol Med* Maywood 2010;235(5):633–41.
34. **Devanur LD, Evans RW, Evans PJ, et al.** Chelator-facilitated removal of iron from transferrin: relevance to combined chelation therapy. *Biochem J* 2008;409(2):439–47.
35. **Vlachodimitropoulou Koumoutsea E, Garbowski M, Porter J.** Synergistic intracellular iron chelation combinations: mechanisms and conditions for optimizing iron mobilization. *Br J Haematol* 2015;170(6):874–83.
36. **Peyssonaux C, Zinkernagel AS, Schuepbach RA, et al.** Regulation of iron homeostasis by the hypoxia-inducible transcription factors (HIFs). *J Clin Invest* 2007;117(7):1926–32.
37. **Halberg N, Khan T, Trujillo ME, et al.** Hypoxia-inducible factor 1 α induces fibrosis and insulin resistance in white adipose tissue. *Mol Cell Biol* 2009;29(16):4467–83.
38. **Higgins DF, Kimura K, Bernhardt WM, et al.** Hypoxia promotes fibrogenesis in vivo via HIF-1 stimulation of epithelial-to-mesenchymal transition. *J Clin Invest* 2007;117(12):3810–20.
39. **Moon J-O, Welch TP, Gonzalez FJ, et al.** Reduced liver fibrosis in hypoxia-inducible factor-1 α -deficient mice. *Am J Physiol Gastrointest Liver Physiol* 2009;296(3):G582–92.

From the Regeneration and Repair Group (KJM, JDC, MBO, PPM, RW, WKS), The Institute of Hepatology, Foundation for Liver Research, London, UK; Faculty of Life Sciences & Medicine (KJM, JDC, MBO, PPM, WKS), King's College London, London, UK; Department of Biomedical Sciences (KJM, VBP), University of Westminster, London, UK; Division of Gastroenterology and Hepatology (PPM), University Hospital Essen, Essen, Germany; Section of Gastroenterology (WKS), Ralph H Johnson VAMC, Charleston, South Carolina; Department of Medicine (WKS), Medical University of South Carolina, Charleston, South Carolina.

Submitted April 25, 2017; accepted August 21, 2017.

The authors have no conflicts of interest to disclose.

Funding: Foundation for Liver Research (W.K.S.), Polkemmet Trust (W.K.S.), Dunse Foundation/British Liver Trust (W.K.S.).

Correspondence: Wing-Kin Syn, MD, Division of Gastroenterology and Hepatology, Department of Medicine, Medical University of South Carolina, Strom Thurmond Building, 114 Doughty Street, MSC, 702, Room 402, Charleston, SC 29425 (E-mail: synw@muscc.edu).